JCI The Journal of Clinical Investigation

Ca^{2+}-binding protein NECAB2 facilitates inflammatory pain hypersensitivity

Ming-Dong Zhang, … , Tibor Harkany, Tomas Hökfelt

J Clin Invest. 2018. https://doi.org/10.1172/JCI120913.

Research Article In-Press Preview **Neuroscience**

Graphical abstract

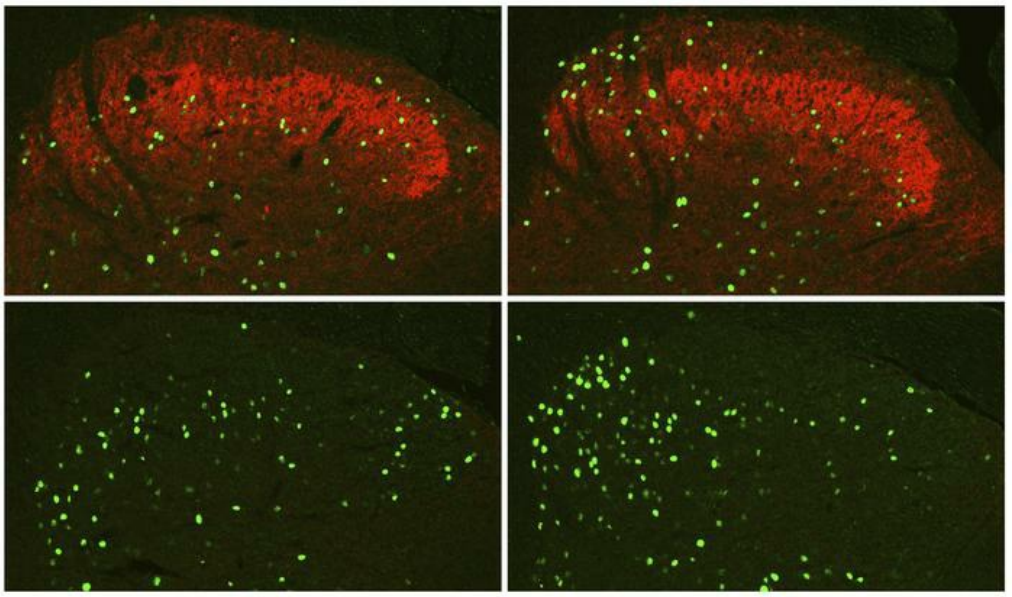

Revised manuscript: 120913-JCI-RG-RV-3

Ca^{2+}-binding protein NECAB2 facilitates inflammatory pain hypersensitivity

Ming-Dong Zhang[1,#,†], Jie Su[1,#,†], Csaba Adori[1], Valentia Cinquina[2], Katarzyna Malenczyk[2], Fatima Girach[2], Changgeng Peng[3], Patrik Ernfors[3], Peter Löw[1], Lotta Borgius[1], Ole Kiehn[1], Masahiko Watanabe[4], Mathias Uhlén[5], Nicholas Mitsios[5], Jan Mulder[5], Tibor Harkany[1,2,*] and Tomas Hökfelt[1,*]

[1]Department of Neuroscience, Karolinska Institutet, SE-17177 Stockholm, Sweden; [2]Department of Molecular Neurosciences, Center for Brain Research, Medical University of Vienna, Spitalgasse 4, A-1090 Vienna, Austria; [3]Division of Molecular Neurobiology, Department of Medical Biochemistry and Biophysics, Karolinska Institutet, SE-17177 Stockholm, Sweden; [4]Hokkaido University School of Medicine, Sapporo 060-8638, Japan and [5]Science for Life Laboratory, Department of Neuroscience, Karolinska Institutet, SE-17177 Stockholm, Sweden.

[#] M.-D. Z. and J. S. contributed equally

* T.Ha. and T. Hö share senior authorship

[†]Present address: Division of Molecular Neurobiology, Department of Medical Biochemistry and Biophysics, Karolinska Institutet, SE-17177 Stockholm, Sweden

Correspondence should be addressed to:

Dr. **Tibor Harkany**, Department of Molecular Neurosciences, Center for Brain Research, Medical University of Vienna, Spitalgasse 4, A-1090 Vienna, Austria; *tel*: +43 1 40160 34050; *e-mail*: tibor.harkany@meduniwien.ac.at - or -

Dr. **Tomas Hökfelt**, Department of Neuroscience, Retzius väg 8, Karolinska Institutet, SE-17177 Stockholm, Sweden; *tel*: +46 8 524 87070; *e-mail*: tomas.hokfelt@ki.se

Conflict of Interest

The authors have declared that no conflict of interest exists.

Abstract

Painful signals are transmitted by mutisynaptic glutamatergic pathways. Their first synapse between primary nociceptors and excitatory spinal interneurons gates sensory load. Glutamate release herein is orchestrated by Ca^{2+} sensor proteins with neuronal calcium-binding protein 2 (NECAB2) being particularly abundant. However, neither the importance of $NECAB2^{+}$ neuronal contingents in dorsal root ganglia (DRG) and spinal cord nor function-determination by NECAB2 has been defined. A combination of histochemistry and single-cell RNA-seq showed NECAB2 in small/medium-sized C- and Aδ D-hair low threshold mechanoreceptors in DRG, as well as in protein kinase γ-positive excitatory spinal interneurons. NECAB2 was downregulated by peripheral nerve injury, offering the hypothesis that NECAB2 loss-of-funtion could limit pain sensation. Indeed, $Necab2^{-/-}$ mice reached a pain-free state significantly faster after peripheral inflammation than wild-type littermates. Genetic access to transiently-activated neurons revealed that a mediodorsal cohort of $NECAB2^{+}$ neurons mediates inflammatory pain in mouse spinal dorsal horn. Here, besides dampening excitatory transmission in spinal interneurons, NECAB2 limited pronociceptive brain-derived neurotrophic factor release from sensory afferents. Hox8b-dependent reinstatement of NECAB2 expression in $Necab2^{-/-}$ mice then demonstrated that spinal/DRG NECAB2 alone could control inflammation-induced sensory hyperensitivity. Overall, we identify NECAB2 as a critical component of pro-nociceptive pain signaling whose inactivation offers substantial pain relief.

Key words: Ca^{2+}-binding protein, genetic circuit mapping, light-sheet microscopy, neurochemical heterogeneity, pro-inflammatory cytokine.

Introduction

Acute pain (nociception) is a physiologically-relevant sensation aimed at alerting to and thus limiting tissue damage on environmental impact. In turn, chronic pain is the consequence of a series of maladaptive responses following tissue or nerve damage (1, 2). Chronic pain is a rising health problem afflicting around 20% of European adults (3) with treatment options still largely limited to opioids and non-steroidal anti-inflammatory drugs (4-6), and led to an 'opiate epidemic' given the addictive side-effects and escalated regime of opioid drugs (4, 7). This is despite detailed insights in cellular determinants of both neuropathic and inflammatory pain becoming available (8-20), and motivating drug development (21) ever since Melzack and Wall's introduction of the 'gate control theory' of pain (10).

Ca^{2+} signaling regulates neurotranmistter release at every presynapse of the nervous system (22) by priming the SNARE machinery to allow the exocytosis of neurotransmitter-laden vesicles. Amongst SNARE proteins, synaptotagmin I binds Ca^{2+} (with its C2 domains) and thus is an essential Ca^{2+}-sensor converting neuronal activity into fast vesicle release (23). N-terminal EF-hand Ca^{2+}-binding proteins 1-3 (NECAB1-3) are highly homologous members of a family of Ca^{2+} sensors that unconventionally contain only a single EF-hand domain for Ca^{2+} binding. NECAB1 interacts with synaptotagomin I at its C2A-domain that also binds syntaxin I at high affinity, even if only trace amounts of Ca^{2+} are present (24). NECAB1 and NECAB2 are expressed in neurons (henceforth also termed 'neuronal Ca^{2+}-binding proteins') with particularly notable expression in dorsal root ganglia (DRGs) and mainly excitatory interneurons in the spinal cord (25). NECAB1 and NECAB2 expression patterns are conserved across mammals (25, 26), highlighting the relevance of their study for human pathologies. Single-cell RNA-sequencing (RNA-seq) assigned *Necab2* as a marker of thinly myelinated neurons otherwise co-expressing ($^+$) neurotrophin receptor tyrosine kinase 2 (*Ntrk2*)/neurofilament heavy chain (*Nefh*) in mouse DRG (27, 28). Since *Ntrk2*$^+$ sensory neurons could contribute to the development of neuropathic pain (besides mediating light touch sensation physiologically) (16), an unanswered yet critical question is if NECAB2 in these sensory neurons is of functional importance. This is particularly relevant for NECAB2 since, unlike NECAB1, it is regulated at the DRG level by peripheral axotomy (25). However, it is unclear if the plasticity of NECAB2 in response to peripheral nerve injury indicates molecular adaptation or affords causality by reducing pro-nociceptive neurotransmission.

Here, we sought to address the role of NECAB2 in pain circuits at the DRG and spinal levels by combining models for neuropathic and inflammatory pain, behavioral phenotyping, and circuit reconstruction by histochemistry, biochemistry and genetic access to pain-activated neurons in *Necab2*$^{-/-}$ and wild-type mice. Our analysis reveals that NECAB2 marks C- and Aδ D-hair low threshold mechanoreceptive sensory neurons (LTMR) and excitatory protein kinase Cγ$^+$ spinal interneurons. We also show that NECAB2 loss-of-function (*Necab2*$^{-/-}$) in glutamatergic (excitatory) pathways facilitates behavioral recovery, in a large bart by decreasing the production and release of brain-derived neurotrophic factor (BDNF) and pro-

inflammatory cytokines upon inflammation. Conversely, genetic rescue of *Necab2* at the spinal level is sufficient to reinstate wild-type-like pain sensitivity, designating NECAB2 as a critical molecular determinant of pro-nociceptive neurotransmission.

Results

NECAB2 localization in DRG and spinal cord

We sought precise information on the localization of NECAB2 in the DRG and spinal cord by combining high-resolution histochemistry and single-cell RNA-seq. First, we have applied a novel high-sensitivity antibody against NECAB2 (HPA014144) to show that 33 ± 2% of DRG neurons, mainly small- and medium-sized ones, express this Ca^{2+} sensor protein (Figure 1A,B). These neurons were essentially neither peptidergic (4 ± 1% co-localization with calcitonin gene-related peptide [CGRP]) nor non-peptidergic (4 ± 2%, iso-lectin $B4^+$ [IB4]) (Figure 1C,D). Likewise, NECAB2 showed complementarity with calbindin D28k (barring a few exceptions, Figure 1G) and secretagogin (Figure 1H), respective Ca^{2+}-binding and alternative Ca^{2+}-sensor proteins expressed in DRG (29). Next, we asked if $NECAB2^+$ sensory neurons harbor the capacity to produce fast neurotransmitters instead: indeed, these cells were often tyrosine hydroxylase$^+$ (TH^+; Figure 1E,L) or neurotrophin receptor tyrosine kinase B^+ ($TrkB^+$; Figure 1F,L), which by combined single-cell RNA-seq (Figure 1L) and function determination (27) qualifies them as C-low and Aδ D-hair LTMRs, respectively. Moreover, single-cell RNA-seq validated the likelihood of *Th*/*Vglut2* (the latter encoding vesicular glutamate transporter 2) co-existence (108 Th^+ cells also contained *Vglut2* mRNA in a pool of 344 *Vglut2*-expressing neurons), reinforcing an association of NECAB2 with excitatory neurotransmission. In fact, small-sized $NECAB2^+$ neurons were $VGLUT2^+$, whereas we could not detect either VGLUT2- or VGLUT1-like immunoreactivity (LI) in medium-sized ones (Figure 1I-K). Finally, we combined *in situ* hybridization and immunohistochemistry in $Necab2^{-/-}$ and wild-type mice to localize *Necab2* mRNA in protein kinase Cγ ($PKC\gamma)^+$ excitatory interneurons in the spinal dorsal horn (Figure 1M-O). Cumulatively, our findings significantly extend available data (25, 30) on the association of NECAB2 to excitatory circuits at the DRG and spinal levels.

Peripheral injury down-regulates NECAB2 expression in sensory neurons

Upon transecting the sciatic nerve (axotomy), the number of $NECAB2^+$ DRG neurons of lumbar 4-6 regions (always used unless stated otherwise) decreased rapidly and persistenly (Figure 2A-C), being significantly different from the contralateral side by 72h post-injury (34 ± 4% [contralateral] *vs*. 13 ± 1% [ipsilateral], $p < 0.01$; Figure 2D). Ipsilateral to the injury, $NECAB2^+$ neurons frequently and transiently (at 24h but not 72h; Figure 2B,C) co-expressed activating transcription factor 3 (ATF3), a nerve injury marker (31).

We then tested if spared nerve injury (SNI), a form of neuropathic pain induction that allows functional analysis (32) affects NECAB2 expression. Indeed, *Necab2* mRNA levels were significantly reduced in DRGs, but not spinal cord, ipsilateral to SNI, as compared to the

contralateral side serving as negative control (1.02 ± 0.22 [contralateral] *vs*. 0.67 ± 0.16 [ipsilateral], $p < 0.05$ for DRG; Figure S1A). SNI also reduced NECAB2 protein levels as detected histochemically and quantitatively expressed as a reduced number of NECAB2$^+$ DRG neurons (34 ± 1% [contralateral] *vs.* 17 ± 5% [ipsilateral, 72h; $p < 0.01$] or 27 ± 1% [ipsilateral, 2 weeks; $p < 0.05$]; Figure 2E-H). NECAB2 expression remained unchanged in ipsilateral spinal cord (Figure S1B,C) even though microglia activation (marked by elevated ionized Ca^{2+}-binding adaptor molecule 1 (Iba1)) was seen in both dorsal and ventral horns, ipsilaterally with focal concentration around motorneurons (Figure S1D). Similar to axotomy, NECAB2$^+$ sensory neurons transiently expressed ATF3 after SNI (0.2 ± 0.3% at 72h, 2 ± 4% after 2 weeks; Figure 2F,G). In sum, NECAB2 expression is significantly and persistently down-regulated in DRG neurons in response to peripheral nerve injury.

Retention of NECAB2 in sensory neurons upon inflammatory pain

Inflammatory pain induced by λ carrageeenan injection into an extremity produces long-lasting hyperalgesia and central sensitization, at least in part, involving C- and Aδ D-hair LTMRs (33). Despite this circuit postulate, λ carrageeenan infusion in a hind-paw affected neither the percentage/distribution nor ATF3 expression of NECAB2$^+$ sensory neurons (30 ± 5% [contralateral] *vs*. 27 ± 3% [ipsilateral]; Figure 2I-L), even though *Necab2* mRNA was notably down-regulated in DRG (1.00 ± 0.08 [contralateral] to 0.80 ± 0.12 [ipsilateral], $p = 0.032$) 72h post-induction (Figure S1E). Likewise, neither *Necab2* mRNA nor protein levels were altered in spinal cord after inflammation (Figure S1E,F). Thus, data from injury and inflammatory models suggest that NECAB2 expression is differentially regulated. This finding raises the possibility that NECAB2 might modulate slow-onset and persistent inflammatory pain whilst undergoing adaptive down-regulation, alike Ca^{2+}/calmodulin-dependent protein kinase type IV (34), upon irreversible physical injury. This hypothesis also suggests differential responsiveness of *Necab2*$^{-/-}$ mice to neuropathic *vs*. inflammatory pain.

NECAB1 does not compensate for NECAB2 in *Necab2*$^{-/-}$ mice

We then sought to address NECAB2 function in pain circuits by generating *Necab2*$^{-/-}$ mice with the promoter-driven knockout first strategy (Figure 3A) (35). By using *Necab2*$^{-/-}$ tissues, we first re-evaluated the specificity of the anti-NECAB2 antibodies available to us: HPA013998, used in our previous study (25), showed residual immunoreactivity in DRGs but not spinal cord of *Necab2*$^{-/-}$ mice (Figure 3B), raising the possibility of its unwanted cross-reactivity with NECAB1 (Figure 3C and SI for discussion). This is plausible even if both the HPA013998 and HPA14144 antibodies labelled bands at the calculated molecular weight of NECAB2 in Western blotting (Figure 3D). These observations highlight that an antibody may show correct staining in one tissue but not another, and underlie the importance of testing antibody specificity for each tissue/organ/system analyzed in knock-out mice (36, 37).

NECABs exist in three isoforms (NECAB1-3) with NECAB1 being the alternative transcript chiefly expressed in the nervous system (23). Therefore, it is plausible that the loss of a NECAB isoform is compensated by another, biasing functional phenotypes. Here, we show that even though *Necab2*$^{-/-}$ mice have elevated *Necab1* mRNA in both DRG and spinal cord (Figure S2A), this does not translate into increased levels of NECAB1 protein in either structure (Figure S2B-G). We then considered that *Necab2* ablation might modulate VGLUT1-3 expression for glutamate neurotransmission. *Vglut1* mRNA in DRG but not spinal cord (Figure S2H) was significantly increased in *Necab2*$^{-/-}$ mice. Consequently, we detected significantly increased protein levels of VGLUT1, which is transported centrally from DRG neurons (38), in *Necab2*$^{-/-}$ spinal cord (Figure S2I). *Vglut2* mRNAs were also elevated in both DRG and spinal samples of *Necab2*$^{-/-}$ mice (Figure S2H), yet this did not translate into an appreciable increase of the ensuing VGLUT2 protein (Figure S2J). *Vglut3* mRNA levels remained unchanged on *Necab2*$^{-/-}$ background (Figure S2H). Similarly, PKCγ and glutamic acid decarboxylase 65/67 (GAD65/67) protein concentrations remained unchanged in *Necab2*$^{-/-}$ mice, as compared to wild-type littermates (Figure S2K,L). These data justify the analysis of excitatory (pro-nociceptive) pain circuits in *Necab2*$^{-/-}$ mice given that functional recovery could be viewed as counteracting enhanced glutamatergic neurotransmission.

Necab2$^{-/-}$ and *Scgn*$^{-/-}$ mice are sensitive to neuropathic pain

Acute pain sensation (noxious, mechanical stimulus by pinprik) was intact in *Necab2*$^{-/-}$ mice without gender difference (Figure 4A). After SNI, *Necab2*$^{-/-}$ mice also developed tactile allodynia (measured by von Frey filament), mechanical hypersensitivity (pinprik) and cold allodynia (acetone) to an extent equivalent to wild-type littermates (Figure 4B-D). Gender differences could not be detected in the SNI model either. We then analyzed secretagogin null (*Scgn*$^{-/-}$) mice to test if an alternative Ca^{2+}-sensor protein (39) also expressed in DRG (29) would differentially modulate nociception upon neuropathic pain. Similar to *Necab2*$^{-/-}$ mice, *Scgn*$^{-/-}$ animals developed tactile and cold allodynia, as well as mechanical hypersensitivity in the SNI model (Figure 4J-L). Thus, neither Ca^{2+}-sensor protein gates nociceptive information transfer from DRG to ascending centers.

Improved behavioral recovery of *Necab2*$^{-/-}$ but not *Scgn*$^{-/-}$ mice after inflammatory pain

Once inducing inflammation by λ carrageenan, the severity and time course of the development of edema did not differ between *Necab2*$^{-/-}$ and wild-type mice (Figure 4E), with it being pronounced by 6h, peaking between 24-72h and partially reciding by day 7 ($p < 0.05$ ipsilateral *vs*. contralateral paw for each time point during 24h-7 days). Tactile allodynia elcitied by acute inflammatory pain was similarly augmented between *Necab2*$^{-/-}$ and wild-type mice up to 6h (Figure 4F). Yet inflammatory pain in *Necab2*$^{-/-}$ mice was significantly attenuated by 24h (Figure 4G, $p = 0.014$, ipsilateral paw, *Necab2*$^{-/-}$ *vs*. wild-type mice) and reached basal threshold by 72h (Figure 4H,I). Considering that the extent of edema did not differ between the genotypes studied, we infer that reduced pro-nociceptive/excitatory signaling at the DRG and spinal levels

might facilitate behavioral recovery during the phase of pain consolidation in *Necab2*$^{-/-}$ mice. Subsequently, we asked if this phenotype was specific to NECAB2 or could as well be a prototypic response on limiting Ca^{2+}-sensor functionality. As such, tactile allodynia after λ carrageenan-induced inflammatory pain in *Scgn*$^{-/-}$ mice was of the same magnitude as in wild-type controls (Figure 4M). Thus, and contrasting NECAB2, secretagogin does not appear to molecularly gate pro-nociceptive excitation associated with inflammatory pain. Moreover, our findings delineate superficial dorsal laminae in which DRG afferents terminate and innervate (also) NECAB2^{+} excitatory interneurons as a focus of NECAB2-dependent signaling events.

Convergence of inflammatory signals in spinal cord

We gained insights in the extent of the neuronal circuitry that underpins inflammatory pain signaling by using a genetic reporter approach exploiting 'permanent genetic access to transiently active neurons', also termed 'targeted recombination in active (cell) populations' (TRAP) (40), driven by the immediate-early gene *Arc*. We focused on recombination events at the spinal level since *Arc* (alike *Fos*, the alternative and experimentally amenable immediate early gene) seems to be expressed in DRG (41). Peripheral inflammation-induced activation of primary sensory afferents coincident with tamoxifen priming (within a window of 6-12h after λ carrageenan injection) in *Arc-CreER*^{T2}*::ROSA26-stop-ZsGreen* reporter mice (Figure 5A-F; Figure S3A,B) allowed us to show that NECAB2^{+} neurons in laminae I/II of the dorsal spinal horn might have received sufficiently strong synaptic inputs for becoming *ZsGreen*$^{+}$ (Figure 5G,H). Inflammatory pain-induced activation of NECAB2^{+} spinal neurons was reinforced by the histochemical co-localization of NECAB2 and Fos (Figure 5I-L). Alike *Arc*-driven *ZsGreen* expression (Figure 5D), Fos immunoreactivity was mainly seen in medial superficial layers of the spinal cord (Figure 5J,L), with it being significantly more abundant in *Necab2*$^{-/-}$ than wild-type mice (Figure 5M; Figure S3C,D). Our histochemical data were validated by a gradual increase in spinal *Fos* mRNA content in *Necab2*$^{-/-}$ mice, reaching significance by 90 min post-intervention (Figure S3E). These data cumulatively suggest that NECAB2^{+} spinal interneurons are cellular determinants of inflammatory pain, and their enhanced activation in *Necab2*$^{-/-}$ mice reflects increased intrinsic network activity to compensate for their functional incompetence when NECAB2 is genetically ablated. Because of the unchanged NECAB2 levels in DRGs upon λ carrageenan administration (Figure 2), we suggest that, in turn, NECAB2 is not rate-limiting for pro-nociceptive excitatory neurotransmission in primary DRG projections to superficial spinal laminae.

Reduced pro-inflammatory cytokine and BDNF responses in *Necab2*$^{-/-}$ mice

Despite the induction of inflammatory pain (for up to 6h) and paw edema being indistinguishable between *Necab2*$^{-/-}$ and wild-type mice (Figure 4E), their differential network activation at the spinal level suggests probable differences in the levels of pronociceptive mediators that are produced and/or released in an activity-dependent manner. Here, we first assayed *Tnfa*, *Il6* and *Il1b* mRNAs (Figure 6A), and show that their transcriptional activation was significantly

reduced in *Necab2*$^{-/-}$ mice relative to wild-type controls. These data concur with glial activation in neuropathic and inflammatory pain models (42-44) (Figure S1D). Next, we histochemically tested if the expression of BDNF, a neuronal pro-nociceptive sensitizing factor acting through TrkB signaling (45), is altered by 72h upon inflammatory pain induction when mechanical allodynia is significantly improved in *Necab2*$^{-/-}$ mice (Figure 4F). As such, peripheral inflammation significantly increased the number of BDNF^{+} neurons in wild-type DRGs (30 ± 6% [contralateral] *vs*. 45 ± 5% [ipsilateral], $p < 0.05$; Figure 6B,C) along with a robust increase in *Bdnf* mRNA transcript levels (Figure 6D). In contrast, an inflammation-induced increase in BDNF^{+} neurons failed to materialize in *Necab2*$^{-/-}$ mice (31 ± 6% [contralateral] *vs*. 37 ± 4% [ipsilateral]; Figure 6B,C) even though *Bdnf* transcription increased (Figure 6D). Notably, these differences were also evident at the spinal level with *Necab2*$^{-/-}$ mice showing significantly attenuated BDNF immunoreactivity in the ipsilateral dorsal horn, as compared to wild-type mice (Figure 6E,F); even if a hemispheric difference was evident in both genotypes. Taken together, these data suggest that *Necab2* deletion in DRGs attenuates BDNF production and release into the dorsal spinal horn to limit pro-nociceptive excitatory signaling in *Necab2*$^{-/-}$ mice, and could, at least inpart, accelerate functional recovery.

Genetic rescue of NECAB2 expression in spinal cord and DRG reinstates pain sensitivity

NECAB2 is also expressed in hind-, mid- and forebrain regions, including nuclei that tune sensory relay (8, 24). Therefore, we asked if NECAB2 at the spinal level is sufficient to gate pro-nociceptive signaling. To this end, we exploited the tissue-restricted expression of *Hoxb8* (46), a member of the *Antp* homeobox gene family: *Hoxb8* is expressed in spinal cord neurons and glia, as well as in all DRG neurons, whilst sparing the brain apart from the spinal trigeminal nucleus. By crossing the *Necab2*(tm1a) allele (Figure 3A) with *Hoxb8-Flp* mice we have successfully reinstated *Necab2* expression below cervical spinal segment 4 and in DRGs (Figure 7A-F). Whole-tissue imaging by light-sheet microscopy after iDISCO+ processing in combination with histochemistry (47) revealed wild-type-like expression and correct localization for NECAB2 in dorsal spinal horn (Figure 7D,F) of *Hoxb8*-Flp::*Necab2*(tm1a) mice. Genetic rescue of *Necab2* expression also reinstated wild-type-like pain sensitivity: *Hoxb8*-Flp::*Necab2*(tm1a) mice developed tactile allodynia with partial recovery only 7 days after λ carrageenan stimulation (Figure 7G,H), matching the profile of wild-type littermates. Thus, NECAB2 at the spinal level is sufficient to consolidate persistent inflammatory pain.

Discussion

The present study takes advantage of the combination of high-resolution histochemistry and single-cell RNA-seq (27) to molecularly tie NECAB2 expression in DRG to C-LTMRs and Aδ D-hair LTMRs. NECAB2 levels decrease in sensory neurons upon peripheral nerve injury, whether axotomy or SNI. The use of SNI is notable because it allows the determination of functional recovery at high temporal resolution (32); and led us to distinguish roles for NECAB2 when combining nerve injury with genetic loss-, as well as gain-of-function analyses.

Accordingly, NECAB2 is dispensable for the transmission of mechanical but not inflammatory pain. By showing that NECAB2 invariably co-exists with VGLUT2 (48) in glutamatergic synapses in primary afferents, excitatory ($PKC\gamma^+$) interneurons and ascending projections (25), its loss is likely to attenuate excitatory neurotransmission. This is significant since modulating excitation/inhibition balance in spinal circuits can alleviate neuropathic pain (49, 50). The involvement of laminae I/II interneurons of the dorsal spinal horn in transmitting inflammation-related nerve activity is reinforced by our immediate early-gene (*Arc*)-driven genetic labeling ('TRAP') (40). TRAP marks cells, many being $NECAB2^+$, whose activity significantly increased within a 6-12h time window upon λ carrageenan challenge. When inflicting peripheral inflammation in *Necab2*$^{-/-}$ mice, significant facilitation of post-traumatic recovery was demonstrated, reaching basal pain thresholds (that is, a pain-free state) remarkably faster than wild-type mice. This finding suggests a pro-nociceptive 'gatekeeper' role for NECAB2 with its action confined to at least three levels: *i*) intraganglionic signaling between sensory neurons, *ii*) BDNF (and/or cytokine release even though we do not exclude contribution by glia residing in spinal cord) from nerve endings of primary afferents in the superficial dorsal horn (that is, at the first synapse in the sensory/pain circuit) and *iii*) dorsal horn interneurons.

Peripheral nerve injury is a stimulus sufficiently strong to trigger expressional changes in hundreds of genes in neurons and glia, which assemble into mutimodal pain pathways along the DRG and spinal cord. The combinatorial outcome of genetic modifications in these pain pathways will underpin pain sensation (e.g., stratify severity), as well as determine innate capacity for adaptation and regeneration in response to mechanical insults (51-54). We posit that rapid down-regulation of NECAB2 could severe excitation, thus preventing transition towards the development of chronic pain. This hypothesis emphasizes a critical role for excitatory spinal interneurons, and is molecularly appealing since NECAB2 is enriched in their $VGLUT2^+$ nerve termials (25), a consensus requirement for all Ca^{2+}-sensors regulating the assembly of SNARE complexes for vesicular exocytosis in the presynapse. Besides regulating vesicular docking events, NECAB2's presynaptic signal integration might involve an interaction with metabotropic glutamate receptor type 5 (mGluR5) (55), which is present in afferents to the dorsal horn (56), where presynaptic mGluR5s enhance glutamate release (57). Thus, *Necab2*$^{-/-}$ mice could have attenuated glutamate release and, consequently, reduced circuit excitation in spinal dorsal horn. Accordingly, genetic or pharmacological dampening of presynaptic NECAB2 availability and/or Ca^{2+} sensitivity in glutamatergic presynapses could protect against excessive pain.

Amongst the many genes up-regulated by synaptic enhancement in laminae I/II are *Arc* and *Fos*, rapidly and transiently expressed immediate early genes. However, neither gene is activated in the DRG (41, 58-60), validating the lack of *ZsGreen* label in TRAP mice upon pain induction (*data not shown*). Considering that Arc and Fos are reliable markers of spinal neurons (61, 62), our experiments outline a dorsomedial domain in laminae I/II of the dorsal horn, which contains the bulk of neurons synaptically activated upon inflammatory pain (Figure 5D,L). Our genetic approach utilizes *Arc* actvation to mark cellular contingents that respond to

inflammatory pain in a binary “yes/no” fashion. Nonetheless, genetic TRAP in this case is insufficient to either correlate Arc/Fos levels and pain-like behaviors or infer the importance of Fos as immediate early gene for pain sensation (58, 63, 64). In sum, our histochemical and genetic circuit-mapping data cumulatively highlight spinal interneurons whose activation is significantly exacerbated upon *Necab2* deletion. If these are interneurons that reduce circuit excitability then their activation could attenuate inflammatory pain sensation. Despite the clear dichotomy of *Necab2* involvement in neuropathic *vs*. inflammatory pain, we cannot entirely negate that up-regulation of *Vglut2* in DRG and spinal cord at the mRNA level upon mechanical stimuli could compensate for and thus, phenotypically mask NECAB2 loss-of-function.

Pro-inflammatory cytokines, like TNFα, IL-6 and IL-1β, induce inflammatory pain upon being released from immune cells through local sensitization of nociceptors (43, 65-68). Similarly, such cytokines cause pain when released by glial cells in the spinal cord following peripheral inflammation (44, 69-72). In *Necab2*$^{-/-}$ mice, the inflammation-induced spinal expression of *Tnfa*, *Il6* and *Il1b* mRNAs was lower than in wild-type mice. Even though we did not address if and how *Necab2* deletion limits microglia activation (and thus neuroinflammation), translating cytokine mRNA levels into reduced tissue TNFα, IL6 or IL1B content outlines a candidate mechanism to attenuate inflammatory pain. Likewise, λ carrageenan application increased the expression of BDNF, an accepted marker of peripheral inflammation . BDNF is an essential growth factor during nervous system development (73) and modulates synaptic neurotransmission in adult (74). BDNF is expressed by peptidergic nociceptors, stored in large dense-core vesicles (often together with neuropeptides), and released from both A- and C-fibers in spinal superficial layers (75, 76). BDNF binding to TrkB receptors then triggers central sensitization, including postsynaptic NMDA receptor activation and downstream *Fos* mRNA expression (77-79). Therefore, inhibiting BDNF signaling at the spinal level can reduce progressive (but not acute) inflammatory pain and heat hypersensitivity (45, 80, 81). Our data prompt the suggestion that both BDNF and NECAB2 are presynaptic determinants of glutamatergic hyperactivity upon persistent pain with BDNF modulating postsynaptic receptor accessibility and/or hypersensitivity (e.g. NMDA receptors), whereas NECAB2 scaling glutamate and BDNF release from excitatory nerve terminals. Here, we show that *Necab2*$^{-/-}$ mice fail to respond to inflammatory stimuli by increasing BDNF in primary afferents in laminae I/II, an observation that defines a DRG-locked mechanism for NECAB2. Consequently, attenuated BDNF (and probably cytokine) singaling in spinal superficial layers of *Necab2*$^{-/-}$ mice can curtail circuit hypersensitivity and thus, promote recovery after inflammation. Even though BDNF is primarily associated with excitatory neurotransmission, data exist on glia-derived BDNF production and focal release upon injury (82-85). Therefore, and despite that Iba1^{+} microglia were BDNF^{-} in our wild-type specimens, we cannot entirely rule out an effect, however indirect, of *Necab2* deletion on attenuated BDNF production in microglia upon peripheral inflammation. In sum, inhibition of coincidently occluding NECAB2-mediated vesicular glutamate and BDNF exocytosis in excitatory spinal interneurons, BDNF/TrkB^{+}/VGLUT2^{+} DRG neurons (77, 86), and perhaps resident microglia, could prove particularly efficient to limit pain

signaling brought about by peripheral inflammation. Our assertion is compatible with recent patent literature with NECAB2 named as a biomarker and prospective druggable target for rheumatoid arthritis and multiple sclerosis.

There are efficient endogenous mechansims to defend against persistent pain, particularly with inflammatory origins. In addition to descending systems (87), local dorsal horn neurons expressing opioid peptides that suppress pain signaling via their cognate receptor systems (88, 89). Opioid receptors are therefore preferred targets for many analgesic drugs, the most efficient being morphine. Neuropathic pain, which results from a more instantaneous insult, is controlled by modulating DRG sensory neurons through, e.g. the 29 amino acid-long peptide galanin (90). The present report reconciles the above difference of action by identifying pronociceptive NECAB2 as a molecular determinant of inflammatory pain at the DRG and spinal interneuron levels, with its downregulation being causal to preventing persistent pain and to facilitating functional recovery. The presynaptic site of action for NECAB2 is of benefit to also dampen BDNF release directly and iinflammatory cytokine production indirectly in the spinal cord, thus producing a palette of coordinated actions to reduce the coincident and activity-dependent release of fast neurotransmitters and pro-inflammatory neuromodulators from DRG afferents and excitatory spinal interneurons. These findings seem significant to meet the unment need of therapies beyond opiates in today's epidemic particularly since chronic inflammatory pain affects 1.7-5% of the general population (vs. 8% suffering from chronic neuropathic pain) (9, 91-93).

Materials and Methods

Animals. Wild-type (WT) male C57BL/6 mice (adult, ~15 weeks of age) were obtained from Charles River (Scanbur AB). *Necab2* and *Scgn* knock-out first, promoter driven mice were custom-generated by the Knockout Mouse Project (KOMP) Repository at UCDAVIS. *Hoxb8-Flp*, *Vglut2::*EGFP and *Arc-Cre*$^{ERT/2}$::ROSA26-stop-*ZsGreen1* mice were from licenced resources. Animals were kept under standard conditions, including a 12/12-h light-dark cycle with *ad libitum* access to food and water. Efforts were made to minimize the number of mice used and their suffering throughout.

Surgery. Complete transection of the sciatic nerve (axotomy) at mid-thigh level of the hind-leg was performed as described earlier (94). Spared nerve injury (SNI) was carried out according to published protocols (32, 95). For the carrageenan model, mice received an intra-plantar injection of 1% λ carrageenan (in 20 µl volume, Sigma) in the hind paw (28G needle) (96) (SI Materials and Methods).

Tamoxifen-induced TRAP. Tamoxifen was dissolved in corn oil (Sigma) and injected subcutaneously (150-200 mg/kg, Sigma) in *Arc*TRAP mice 12 h before 1% λ carrageenan infusion (40, 97). *Arc*TRAP mice (vehicle and carrageenan) were perfused after either 6h or 72h of the onset of inflammation, with the latter being particularly suited to allow increased cellular ZsGreen1 content in activated cell populations. Mice with 72h survival received subsequent tamoxifen doses daily.

Behavioral assessment. Withdrawal threshold was tested in transparent plastic domes on a metal mesh floor and measured by a logarithmically incremental stiffness of 0.04, 0.07, 0.16, 0.40, 0.60, 1.0, and 2.0 (g) von Frey filament (Stoelting) combined with an up-down method to assess tactile allodynia (32, 98, 99). For mechanical hyperalgesia, a safety pin was used and the duration of paw withdrawal was recorded (32). Cold allodynia was tested with a drop of acetone with the duration of the withdrawal response recorded (32).

Quantitative real time-PCR (qPCR). Total RNA was isolated and extracted by using TRI Reagent (Sigma-Aldrich). qPCR reactions were performed using Maxima SYBR Green Master Mix with ROX (Thermo Scientific) on an Applied Biosystems QuantStudio5 unit. Primer pairs were listed in Table S1 (SI Materials and Methods).

Western blotting. Total protein samples were extracted from freshly dissected DRGs and spinal cord of WT and *Necab2* knockout mice using radioimmunoprecipitation assay lysis buffer and subjected to Western blotting as described (25) (*SI Materials and Methods*).

Tissues and immunohistochemistry. For immunohistochemstry, mice were deeply anesthetized and transcardially perfused with 4% paraformaldehyde (29) (*SI Materials and Methods*). Primary antibodies used in this study are referred to in Table S2 (*SI Materials and Methods*).

In situ hybridization and immunohistochemistry. Spinal cord cryosections (20 μm, as above) were processed, and hybridized as previously described with minor modifications (100). Digoxigenin (DIG)-labelled *Necab2* RNA probe was used (26). Subsequently, alkaline-phosphatase-conjugated anti-digoxigenin antibody (goat antibody, 1: 2,000, Roche) was applied and developed with Fast Red (Roche). Post-hybridization immunostaining for PKCγ (rabbit antibody, 1:100) was visualized with Alexa Fluro488-conjugated affinity-purified donkey anti-rabbit IgG (1:100; Jackson ImmunoResearch) at 22-24 ^{o}C for 2 h. After rinsing, sections were coverslipped with 1,4-Diazabicyclo[2.2.2]octane (DABCO, Sigma).

Microscopy and image processing. Representative images were acquired on a Zeiss LSM700 confocal laser-scanning microscope (Carl Zeiss) at 1 airy unit pinhole settings and processed in ZEN2012 (Zeiss). Multi-panel figures were assembled with Adobe Photoshop CS6 (Adobe Systems) (*SI Materials and Methods*).

Quantitative morphometry. Quantification of NPs in DRGs, fluorescence intensity in DRGs and spinal cord, and size distribution analysis were performed on tile-scanned images captured on a Zeiss LSM700 laser-scanning microscope (30) (*SI Materials and Methods*).

iDISCO^{+} and volume imaging. iDISCO^{+} tissue clearing, immunostaining and volume imaging processes were performed as described (47) (*SI Materials and Methods*).

Single-cell RNA-seq. Expression data on DRG neurons were re-processed using the dataset published by Usoskin *et al* (27). Accession number: GSE59739.

Statistics. Behavioral data (e.g., von Frey filament test) lacking normal distribution were presented as medians ± interquartile ranges and assessed by the Mann-Whitney *U* test. For pinprick and acetone stimuli, data were expressed as means ± S.D. and evaluated by using unpaired two-tailed Student's *t*-test (Prism 6 software; GraphPad). Data for qPCR, Western blotting and immunohistochemistry were presented as means ± S.D. and also processed by two-tailed Student's *t*-test (nerve injury and inflammation models in WT mice) or two-way ANOVA with Bonferroni's or Tukey's multiple comparisons *post-hoc* analysis where relevant (e.g. genotype on inflammation). A p value of < 0.05 was considered statistically significant.

Study approval. Experiments on laboratory rodents were compliant to Swedish regulations and approved by the regional ethical committee (Stockholms Norra Djurföröksetiska Nämnd, N16/15 and N101/14).

Author contributions

M.D.Z., T.Ha. and T.Hö designed experiments, M.D.Z., J.S., C.A., V.C., C.P. performed experiments and analyzed data; K.M., F.G., P.L., L.B., O.K., M.W., M.U., N.M, J.M developed and provided unique reagents, model systems and experimental tools; P.E., O.K., M.U., T.Ha. and T.Hö. procured funding for this work. M.D.Z., T.Ha. and T.Hö. wrote the manuscript. All authors commented on and approved the submission of this work.

Acknowledgements

We thank Profs. Ingrid Nylander (Uppsala University, Uppsala, Sweden) and Lars Terenius (Karolinska Institutet, Stockholm, Sweden) for generously supplying the CGRP antiserum, as well as Ms. Natalie Sleiers (Karolinska Institutet, Stockholm, Sweden) and Dr. Tony Jimenez-Beristain (Science for Life Laboratory, Solna, Sweden) for their help with *Vglut2::*EGFP and *Necab2*$^{-/-}$ colonies. Laser-scanning microscopy was made available by the Center for Live Imaging of Cells core facility at Karolinska Institutet, supported by the Knut and Alice Wallenberg Foundation. Support for this study was provided by the Swedish Medical Research Council (T.Ha., T.Hö. and O.K.); Karolinska Institutet partial financing scheme of graduate students (T.Ha., T.Hö.); Novo Nordisk Foundation (T.H., T.Hö.), the European Research Council (ERC advanced grants, T.Ha., O.K.), the Swedish Brain Foundation (T.Ha., T.Hö.) and the European Commission's 7th Framework Programme: 'PAINCAGE' integrated grant (T.Ha., T.Hö.).

References

1. Woolf CJ. What is this thing called pain? *J Clin Invest.* 2010;120(11):3742-4.
2. Woolf CJ. Generation of acute pain: central mechanisms. *Br Med Bull.* 1991;47(3):523-33.
3. van Hecke O, Torrance N, and Smith BH. Chronic pain epidemiology and its clinical relevance. *Br J Anaesth.* 2013;111(1):13-8.
4. Grosser T, Woolf CJ, and FitzGerald GA. Time for nonaddictive relief of pain. *Science.* 2017;355(6329):1026-7.
5. Dowell D, Haegerich TM, and Chou R. CDC Guideline for Prescribing Opioids for Chronic Pain--United States, 2016. *JAMA.* 2016;315(15):1624-45.
6. Moore RA, Derry S, Simon LS, and Emery P. Nonsteroidal anti-inflammatory drugs, gastroprotection, and benefit-risk. *Pain Pract.* 2014;14(4):378-95.
7. Majumdar S, and Devi LA. Strategy for making safer opioids bolstered. *Nature.* 2018;553(7688):286-8.
8. Basbaum AI, Bautista DM, Scherrer G, and Julius D. Cellular and molecular mechanisms of pain. *Cell.* 2009;139(2):267-84.
9. Ji RR, Xu ZZ, and Gao YJ. Emerging targets in neuroinflammation-driven chronic pain. *Nat Rev Drug Discov.* 2014;13(7):533-48.
10. Melzack R, and Wall PD. Pain mechanisms: a new theory. *Science.* 1965;150(3699):971-9.
11. Braz J, Solorzano C, Wang X, and Basbaum AI. Transmitting pain and itch messages: a contemporary view of the spinal cord circuits that generate gate control. *Neuron.* 2014;82(3):522-36.
12. Woolf CJ, and Salter MW. Neuronal plasticity: increasing the gain in pain. *Science.* 2000;288(5472):1765-9.
13. Julius D, and Basbaum AI. Molecular mechanisms of nociception. *Nature.* 2001;413(6852):203-10.
14. Woolf CJ. Evidence for a central component of post-injury pain hypersensitivity. *Nature.* 1983;306(5944):686-8.
15. Hokfelt T, Kellerth JO, Nilsson G, and Pernow B. Substance p: localization in the central nervous system and in some primary sensory neurons. *Science.* 1975;190(4217):889-90.
16. Peng C, Li L, Zhang MD, Bengtsson Gonzales C, Parisien M, Belfer I, et al. miR-183 cluster scales mechanical pain sensitivity by regulating basal and neuropathic pain genes. *Science.* 2017;356(6343):1168-71.
17. Xanthos DN, and Sandkuhler J. Neurogenic neuroinflammation: inflammatory CNS reactions in response to neuronal activity. *Nat Rev Neurosci.* 2014;15(1):43-53.
18. Scholz J, and Woolf CJ. The neuropathic pain triad: neurons, immune cells and glia. *Nat Neurosci.* 2007;10(11):1361-8.
19. Basbaum AI, and Woolf CJ. Pain. *Curr Biol.* 1999;9(12):R429-31.
20. Bessou P, and Perl ER. Response of cutaneous sensory units with unmyelinated fibers to noxious stimuli. *J Neurophysiol.* 1969;32(6):1025-43.
21. Yekkirala AS, Roberson DP, Bean BP, and Woolf CJ. Breaking barriers to novel analgesic drug development. *Nat Rev Drug Discov.* 2017;16(8):545-64.
22. Sudhof TC. The presynaptic active zone. *Neuron.* 2012;75(1):11-25.
23. Sudhof TC. Synaptotagmins: why so many? *J Biol Chem.* 2002;277(10):7629-32.
24. Sugita S, Ho A, and Sudhof TC. NECABs: a family of neuronal Ca(2+)-binding proteins with an unusual domain structure and a restricted expression pattern. *Neuroscience.* 2002;112(1):51-63.
25. Zhang MD, Tortoriello G, Hsueh B, Tomer R, Ye L, Mitsios N, et al. Neuronal calcium-binding proteins 1/2 localize to dorsal root ganglia and excitatory spinal neurons and are regulated by nerve injury. *Proc Natl Acad Sci USA.* 2014;111(12):E1149-58.
26. Zhang MD, Barde S, Szodorai E, Josephson A, Mitsios N, Watanabe M, et al. Comparative anatomical distribution of neuronal calcium-binding protein (NECAB) 1 and -2 in rodent and human spinal cord. *Brain Struct Funct.* 2016;221(7):3803-23.

27. Usoskin D, Furlan A, Islam S, Abdo H, Lonnerberg P, Lou D, et al. Unbiased classification of sensory neuron types by large-scale single-cell RNA sequencing. *Nat Neurosci.* 2015;18(1):145-53.

28. Li CL, Li KC, Wu D, Chen Y, Luo H, Zhao JR, et al. Somatosensory neuron types identified by high-coverage single-cell RNA-sequencing and functional heterogeneity. *Cell Res.* 2016;26(1):83-102.

29. Shi TJ, Xiang Q, Zhang MD, Tortoriello G, Hammarberg H, Mulder J, et al. Secretagogin is expressed in sensory CGRP neurons and in spinal cord of mouse and complements other calcium-binding proteins, with a note on rat and human. *Mol Pain.* 2012;8:80.

30. Zhang MD, Barde S, Yang T, Lei B, Eriksson LI, Mathew JP, et al. Orthopedic surgery modulates neuropeptides and BDNF expression at the spinal and hippocampal levels. *Proc Natl Acad Sci USA.* 2016;113(43):E6686-E95.

31. Tsujino H, Kondo E, Fukuoka T, Dai Y, Tokunaga A, Miki K, et al. Activating transcription factor 3 (ATF3) induction by axotomy in sensory and motoneurons: A novel neuronal marker of nerve injury. *Mol Cell Neurosci.* 2000;15(2):170-82.

32. Decosterd I, and Woolf CJ. Spared nerve injury: an animal model of persistent peripheral neuropathic pain. *Pain.* 2000;87(2):149-58.

33. Francois A, Schuetter N, Laffray S, Sanguesa J, Pizzoccaro A, Dubel S, et al. The Low-Threshold Calcium Channel Cav3.2 Determines Low-Threshold Mechanoreceptor Function. *Cell Rep.* 2015.

34. Ji RR, Shi TJ, Xu ZQ, Zhang Q, Sakagami H, Tsubochi H, et al. Ca2+/calmodulin-dependent protein kinase type IV in dorsal root ganglion: colocalization with peptides, axonal transport and effect of axotomy. *Brain Res.* 1996;721(1-2):167-73.

35. Skarnes WC, Rosen B, West AP, Koutsourakis M, Bushell W, Iyer V, et al. A conditional knockout resource for the genome-wide study of mouse gene function. *Nature.* 2011;474(7351):337-42.

36. Uhlen M, Bandrowski A, Carr S, Edwards A, Ellenberg J, Lundberg E, et al. A proposal for validation of antibodies. *Nat Methods.* 2016;13(10):823-7.

37. Saper CB. An open letter to our readers on the use of antibodies. *J Comp Neurol.* 2005;493(4):477-8.

38. Brumovsky P, Watanabe M, and Hokfelt T. Expression of the vesicular glutamate transporters-1 and -2 in adult mouse dorsal root ganglia and spinal cord and their regulation by nerve injury. *Neuroscience.* 2007;147(2):469-90.

39. Wagner L, Oliyarnyk O, Gartner W, Nowotny P, Groeger M, Kaserer K, et al. Cloning and expression of secretagogin, a novel neuroendocrine- and pancreatic islet of Langerhans-specific Ca2+-binding protein. *J Biol Chem.* 2000;275(32):24740-51.

40. Guenthner CJ, Miyamichi K, Yang HH, Heller HC, and Luo L. Permanent genetic access to transiently active neurons via TRAP: targeted recombination in active populations. *Neuron.* 2013;78(5):773-84.

41. Hunt SP, Pini A, and Evan G. Induction of c-fos-like protein in spinal cord neurons following sensory stimulation. *Nature.* 1987;328(6131):632-4.

42. Ji RR, Chamessian A, and Zhang YQ. Pain regulation by non-neuronal cells and inflammation. *Science.* 2016;354(6312):572-7.

43. McMahon SB, La Russa F, and Bennett DL. Crosstalk between the nociceptive and immune systems in host defence and disease. *Nat Rev Neurosci.* 2015;16(7):389-402.

44. Berta T, Park CK, Xu ZZ, Xie RG, Liu T, Lu N, et al. Extracellular caspase-6 drives murine inflammatory pain via microglial TNF-alpha secretion. *J Clin Invest.* 2014;124(3):1173-86.

45. Mannion RJ, Costigan M, Decosterd I, Amaya F, Ma QP, Holstege JC, et al. Neurotrophins: peripherally and centrally acting modulators of tactile stimulus-induced inflammatory pain hypersensitivity. *Proc Natl Acad Sci USA.* 1999;96(16):9385-90.

46. Witschi R, Johansson T, Morscher G, Scheurer L, Deschamps J, and Zeilhofer HU. Hoxb8-Cre mice: A tool for brain-sparing conditional gene deletion. *Genesis.* 2010;48(10):596-602.

47. Renier N, Adams EL, Kirst C, Wu Z, Azevedo R, Kohl J, et al. Mapping of Brain Activity by Automated Volume Analysis of Immediate Early Genes. *Cell.* 2016;165(7):1789-802.

48. Fremeau RT, Jr., Troyer MD, Pahner I, Nygaard GO, Tran CH, Reimer RJ, et al. The expression of vesicular glutamate transporters defines two classes of excitatory synapse. *Neuron.* 2001;31(2):247-60.

49. Foster E, Wildner H, Tudeau L, Haueter S, Ralvenius WT, Jegen M, et al. Targeted ablation, silencing, and activation establish glycinergic dorsal horn neurons as key components of a spinal gate for pain and itch. *Neuron.* 2015;85(6):1289-304.

50. Braz JM, Sharif-Naeini R, Vogt D, Kriegstein A, Alvarez-Buylla A, Rubenstein JL, et al. Forebrain GABAergic neuron precursors integrate into adult spinal cord and reduce injury-induced neuropathic pain. *Neuron.* 2012;74(4):663-75.

51. Xiao HS, Huang QH, Zhang FX, Bao L, Lu YJ, Guo C, et al. Identification of gene expression profile of dorsal root ganglion in the rat peripheral axotomy model of neuropathic pain. *Proc Natl Acad Sci USA.* 2002;99(12):8360-5.

52. Yang L, Zhang FX, Huang F, Lu YJ, Li GD, Bao L, et al. Peripheral nerve injury induces trans-synaptic modification of channels, receptors and signal pathways in rat dorsal spinal cord. *Eur J Neurosci.* 2004;19(4):871-83.

53. Hokfelt T, Zhang X, and Wiesenfeld-Hallin Z. Messenger plasticity in primary sensory neurons following axotomy and its functional implications. *Trends Neurosci.* 1994;17(1):22-30.

54. Costigan M, Befort K, Karchewski L, Griffin RS, D'Urso D, Allchorne A, et al. Replicate high-density rat genome oligonucleotide microarrays reveal hundreds of regulated genes in the dorsal root ganglion after peripheral nerve injury. *BMC Neurosci.* 2002;3:16.

55. Canela L, Fernandez-Duenas V, Albergaria C, Watanabe M, Lluis C, Mallol J, et al. The association of metabotropic glutamate receptor type 5 with the neuronal Ca2+-binding protein 2 modulates receptor function. *J Neurochem.* 2009;111(2):555-67.

56. Jia H, Rustioni A, and Valtschanoff JG. Metabotropic glutamate receptors in superficial laminae of the rat dorsal horn. *J Comp Neurol.* 1999;410(4):627-42.

57. Park YK, Galik J, Ryu PD, and Randic M. Activation of presynaptic group I metabotropic glutamate receptors enhances glutamate release in the rat spinal cord substantia gelatinosa. *Neurosci Lett.* 2004;361(1-3):220-4.

58. Harris JA. Using c-fos as a neural marker of pain. *Brain Res Bull.* 1998;45(1):1-8.

59. Jasmin L, Gogas KR, Ahlgren SC, Levine JD, and Basbaum AI. Walking evokes a distinctive pattern of Fos-like immunoreactivity in the caudal brainstem and spinal cord of the rat. *Neuroscience.* 1994;58(2):275-86.

60. Menetrey D, Gannon A, Levine JD, and Basbaum AI. Expression of c-fos protein in interneurons and projection neurons of the rat spinal cord in response to noxious somatic, articular, and visceral stimulation. *J Comp Neurol.* 1989;285(2):177-95.

61. Renier N, Wu Z, Simon DJ, Yang J, Ariel P, and Tessier-Lavigne M. iDISCO: a simple, rapid method to immunolabel large tissue samples for volume imaging. *Cell.* 2014;159(4):896-910.

62. Coggeshall RE. Fos, nociception and the dorsal horn. *Prog Neurobiol.* 2005;77(5):299-352.

63. Todd AJ, Spike RC, Brodbelt AR, Price RF, and Shehab SA. Some inhibitory neurons in the spinal cord develop c-fos-immunoreactivity after noxious stimulation. *Neuroscience.* 1994;63(3):805-16.

64. Noguchi K, Kowalski K, Traub R, Solodkin A, Iadarola MJ, and Ruda MA. Dynorphin expression and Fos-like immunoreactivity following inflammation induced hyperalgesia are colocalized in spinal cord neurons. *Brain Res Mol Brain Res.* 1991;10(3):227-33.

65. Talbot S, Foster SL, and Woolf CJ. Neuroimmunity: Physiology and Pathology. *Annu Rev Immunol.* 2016;34:421-47.

66. Ghasemlou N, Chiu IM, Julien JP, and Woolf CJ. CD11b+Ly6G- myeloid cells mediate mechanical inflammatory pain hypersensitivity. *Proc Natl Acad Sci USA.* 2015;112(49):E6808-17.

67. Rocha AC, Fernandes ES, Quintao NL, Campos MM, and Calixto JB. Relevance of tumour necrosis factor-alpha for the inflammatory and nociceptive responses evoked by carrageenan in the mouse paw. *Br J Pharmacol.* 2006;148(5):688-95.

68. Cunha FQ, Poole S, Lorenzetti BB, and Ferreira SH. The pivotal role of tumour necrosis factor alpha in the development of inflammatory hyperalgesia. *Br J Pharmacol.* 1992;107(3):660-4.

69. Suter MR, Wen YR, Decosterd I, and Ji RR. Do glial cells control pain? *Neuron Glia Biol.* 2007;3(3):255-68.

70. Narita M, Shimamura M, Imai S, Kubota C, Yajima Y, Takagi T, et al. Role of interleukin-1beta and tumor necrosis factor-alpha-dependent expression of cyclooxygenase-2 mRNA in thermal hyperalgesia induced by chronic inflammation in mice. *Neuroscience.* 2008;152(2):477-86.

71. Xu ZZ, Zhang L, Liu T, Park JY, Berta T, Yang R, et al. Resolvins RvE1 and RvD1 attenuate inflammatory pain via central and peripheral actions. *Nat Med.* 2010;16(5):592-7.

72. Lampa J, Westman M, Kadetoff D, Agreus AN, Le Maitre E, Gillis-Haegerstrand C, et al. Peripheral inflammatory disease associated with centrally activated IL-1 system in humans and mice. *Proc Natl Acad Sci USA.* 2012;109(31):12728-33.

73. Barde YA, Edgar D, and Thoenen H. Purification of a new neurotrophic factor from mammalian brain. *EMBO J.* 1982;1(5):549-53.

74. Thoenen H. Neurotrophins and neuronal plasticity. *Science.* 1995;270(5236):593-8.

75. Michael GJ, Averill S, Nitkunan A, Rattray M, Bennett DL, Yan Q, et al. Nerve growth factor treatment increases brain-derived neurotrophic factor selectively in TrkA-expressing dorsal root ganglion cells and in their central terminations within the spinal cord. *J Neurosci.* 1997;17(21):8476-90.

76. Salio C, Averill S, Priestley JV, and Merighi A. Costorage of BDNF and neuropeptides within individual dense-core vesicles in central and peripheral neurons. *Dev Neurobiol.* 2007;67(3):326-38.

77. Salio C, Lossi L, Ferrini F, and Merighi A. Ultrastructural evidence for a pre- and postsynaptic localization of full-length trkB receptors in substantia gelatinosa (lamina II) of rat and mouse spinal cord. *Eur J Neurosci.* 2005;22(8):1951-66.

78. Garraway SM, Petruska JC, and Mendell LM. BDNF sensitizes the response of lamina II neurons to high threshold primary afferent inputs. *Eur J Neurosci.* 2003;18(9):2467-76.

79. Thompson SW, Bennett DL, Kerr BJ, Bradbury EJ, and McMahon SB. Brain-derived neurotrophic factor is an endogenous modulator of nociceptive responses in the spinal cord. *Proc Natl Acad Sci USA.* 1999;96(14):7714-8.

80. Kerr BJ, Bradbury EJ, Bennett DL, Trivedi PM, Dassan P, French J, et al. Brain-derived neurotrophic factor modulates nociceptive sensory inputs and NMDA-evoked responses in the rat spinal cord. *J Neurosci.* 1999;19(12):5138-48.

81. Groth R, and Aanonsen L. Spinal brain-derived neurotrophic factor (BDNF) produces hyperalgesia in normal mice while antisense directed against either BDNF or trkB, prevent inflammation-induced hyperalgesia. *Pain.* 2002;100(1-2):171-81.

82. Taves S, Berta T, Chen G, and Ji RR. Microglia and spinal cord synaptic plasticity in persistent pain. *Neural Plast.* 2013;2013:753656.

83. Beggs S, and Salter MW. The known knowns of microglia-neuronal signalling in neuropathic pain. *Neurosci Lett.* 2013;557 Pt A:37-42.

84. Ulmann L, Hatcher JP, Hughes JP, Chaumont S, Green PJ, Conquet F, et al. Up-regulation of P2X4 receptors in spinal microglia after peripheral nerve injury mediates BDNF release and neuropathic pain. *J Neurosci.* 2008;28(44):11263-8.

85. Coull JA, Beggs S, Boudreau D, Boivin D, Tsuda M, Inoue K, et al. BDNF from microglia causes the shift in neuronal anion gradient underlying neuropathic pain. *Nature.* 2005;438(7070):1017-21.

86. Salio C, and Ferrini F. BDNF and GDNF expression in discrete populations of nociceptors. *Ann Anat.* 2016;207:55-61.

87. Willis WD, and Westlund KN. Neuroanatomy of the pain system and of the pathways that modulate pain. *J Clin Neurophysiol.* 1997;14(1):2-31.

88. Sandkuhler J. The organization and function of endogenous antinociceptive systems. *Prog Neurobiol.* 1996;50(1):49-81.

89. Dubner R, and Ruda MA. Activity-dependent neuronal plasticity following tissue injury and inflammation. *Trends Neurosci.* 1992;15(3):96-103.

90. Xu XJ, Hokfelt T, and Wiesenfeld-Hallin Z. Galanin and spinal pain mechanisms: past, present, and future. *EXS.* 2010;102:39-50.

91. Fayaz A, Croft P, Langford RM, Donaldson LJ, and Jones GT. Prevalence of chronic pain in the UK: a systematic review and meta-analysis of population studies. *BMJ Open.* 2016;6(6):e010364.

92. Weisman MH, Witter JP, and Reveille JD. The prevalence of inflammatory back pain: population-based estimates from the US National Health and Nutrition Examination Survey, 2009-10. *Ann Rheum Dis.* 2013;72(3):369-73.

93. Hamilton L, Macgregor A, Warmington V, Pinch E, and Gaffney K. The prevalence of inflammatory back pain in a UK primary care population. *Rheumatology (Oxford).* 2014;53(1):161-4.

94. Wall PD, Devor M, Inbal R, Scadding JW, Schonfeld D, Seltzer Z, et al. Autotomy following peripheral nerve lesions: experimental anaesthesia dolorosa. *Pain.* 1979;7(2):103-11.

95. Pertin M, Gosselin RD, and Decosterd I. The spared nerve injury model of neuropathic pain. *Methods Mol Biol.* 2012;851:205-12.

96. Morris CJ. Carrageenan-induced paw edema in the rat and mouse. *Methods Mol Biol.* 2003;225:115-21.

97. Robinson SP, Langan-Fahey SM, Johnson DA, and Jordan VC. Metabolites, pharmacodynamics, and pharmacokinetics of tamoxifen in rats and mice compared to the breast cancer patient. *Drug Metab Dispos.* 1991;19(1):36-43.

98. Bas DB, Su J, Sandor K, Agalave NM, Lundberg J, Codeluppi S, et al. Collagen antibody-induced arthritis evokes persistent pain with spinal glial involvement and transient prostaglandin dependency. *Arthritis Rheum.* 2012;64(12):3886-96.

99. Chaplan SR, Bach FW, Pogrel JW, Chung JM, and Yaksh TL. Quantitative assessment of tactile allodynia in the rat paw. *J Neurosci Methods.* 1994;53(1):55-63.

100. Peng C, Li N, Ng YK, Zhang J, Meier F, Theis FJ, et al. A unilateral negative feedback loop between miR-200 microRNAs and Sox2/E2F3 controls neural progenitor cell-cycle exit and differentiation. *J Neurosci.* 2012;32(38):13292-308.

Figures & Legends

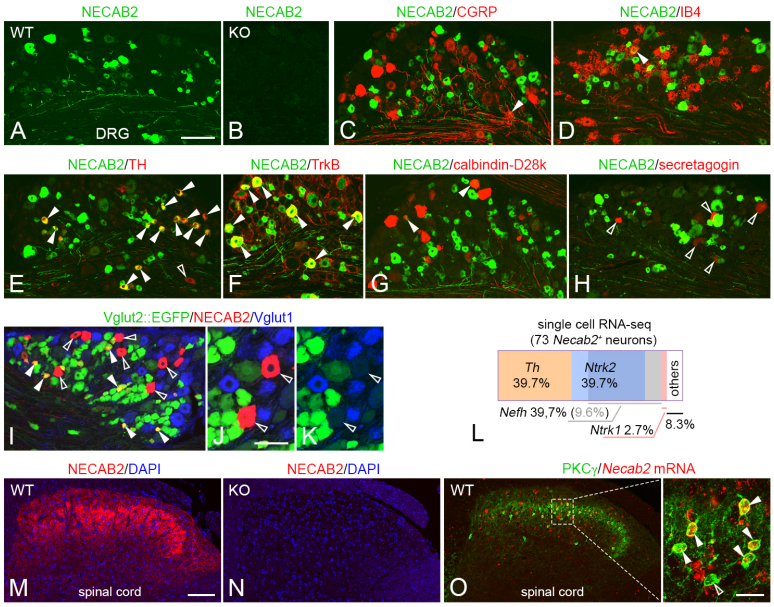

Figure 1. **NECAB2 expression in DRG and spinal cord. A,B**. NECAB2 immunoreactivity in DRGs from wild-type and *Necab2*$^{-/-}$ mice with no residual immunosignal on null background (B). **C,D**. Coincident detection of NECAB2 and CGRP, a peptidergic marker (C), or IB4, a non-peptidergic mark for nociceptors (D). **E,F**. NECAB2 co-exists with TH in C-LTMR (E) or TrkB in Aδ D-hair LTMRs (F). **G,H**. NECAB2 also co-localizes with calbindin D28k (G) but not secretagogin in DRGs (H). **I**. Small-diameter VGLUT2::EGFP but not VGLUT1^{+} neurons harbor NECAB2 in DRGs. **J-K**. Neurochemical heterogeneity of NECAB2^{+} neurons in DRGs. **L**. Molecular phenotyping of *Necab2*-expressing DRG neurons by re-processing open-source single-cell RNA-seq data (26). **M,N**. NECAB2 immunoreactivity in spinal dorsal horn of wild-type mice (L) and its complete loss upon genetic ablation (*Necab2*$^{-/-}$; M). 4,6-diamidino-2-phenylindole (DAPI) was used as nuclear counterstain. **O**. Co-localization of PKCγ and *Necab2* mRNA in excitatory interneurons in spinal dorsal horn. Open dashed rectangle denotes the position of the inset. J,K are projection images from 11-µm thick tissue samples orthogonally scanned with optical steps of 1 µm. Tissues from $n \geq 2$ mice were processed for histochemical analysis. Solid and open arrowheads point to co-localization and the lack thereof, respectively. *Scale bars* = 100 µm (A-I,M,N,O), 20 µm (J,K,O *inset*).

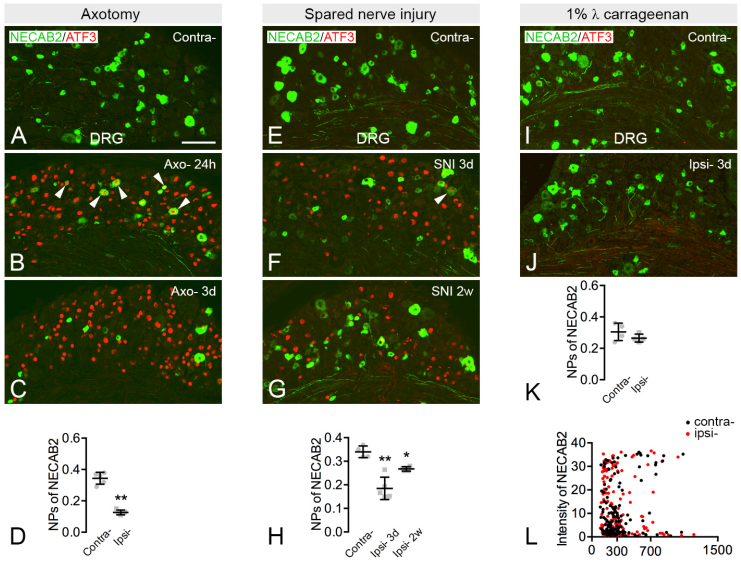

Figure 2. **NECAB2 expression in DRG and spinal cord after peripheral nerve injury and inflammation. A-D**. Double-labeling of NECAB2 and ATF3 in DRG 24h (B) and 3 days (3d, C) after axotomy of the sciatic nerve ('Axo'; *n* = 10 mice/time point), and quantification of neuronal profiles (NPs) for NECAB2 3d post-axotomy ($p < 0.01$). **E-H**. Simultaneous detection and subsequent quantification (H) of NECAB2 and ATF3 in DRG 3d and 2 weeks after spared nerve injury (SNI; *n* = 10 mice/group) revealed a significant loss of neuronal immunoreactivity for NECAB2 ($p < 0.05$, one-way ANOVA) ipsilateral ('Ipsi') to the injury relative to the contralateral side ('contra'). **I-K**. Double-labeling for NECAB2 and ATF3 in DRG 3d after inflammation (1% λ carrageenan) and subsequent quantification of neuronal profiles (NPs) for NECAB2 (*n* = 15 mice/group, Student's *t*-test). **L**. Scatter plot of soma size (μm^2, *x*-axis) *vs.* relative fluorescence intensity (arbitrary units, *y*-axis) for $NECAB2^+$ DRG neurons 3d after inflammation. The number of NPs was expressed as a percentage of the total neuronal number (propidium iodide, PI^+) in DRGs throughout. Data were expressed as means ± S.D. *Scale bars* = 100 µm (A-C, E-G, I and J).

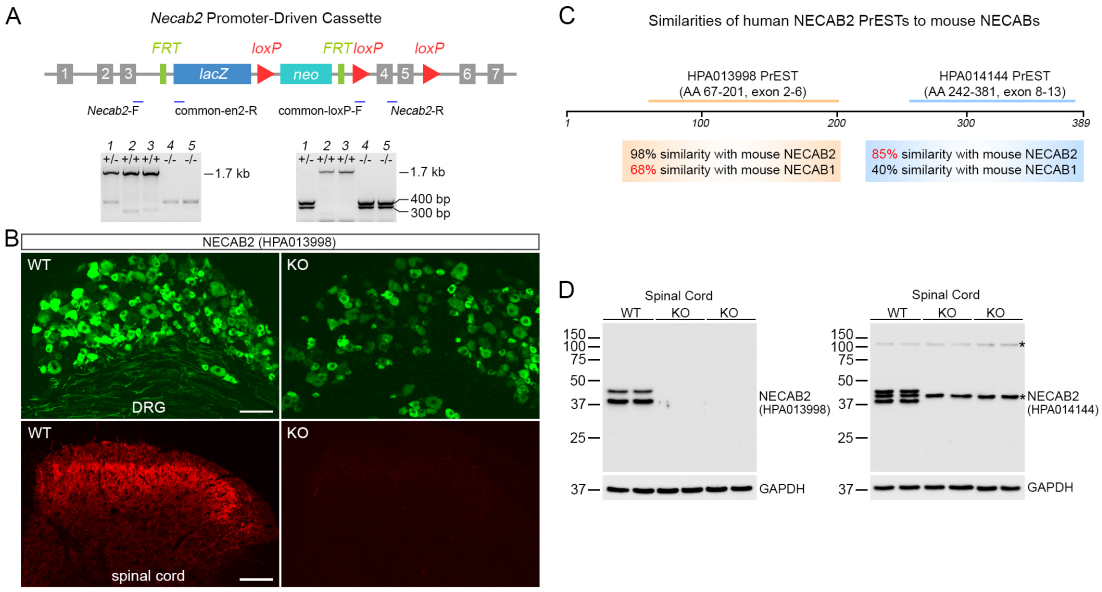

Figure 3. **Generation of *Necab2*$^{-/-}$ mice and antibody validation. A**. Construct for knockout-first, promoter-driven *Necab2*$^{-/-}$ [*Necab2* (tm1a)] mice. Primers (blue lines indicate locations) used for genotyping are shown together with PCR products from wild-type (lanes 2 and 3), heterozygous (lane 1) and *Necab2*$^{-/-}$ offspring (lanes 4 and 5). **B**. Staining pattern of previously used anti-NECAB2 antibody (HPA013998) in DRGs (green) and spinal cord (red) of wild-type (WT) and *Necab2*$^{-/-}$ mice. **C**. Comparison of human NECAB2 protein epitope signature tags (PrESTs) with mouse NECAB1 and NECAB2. **D**. Western blotting of NECAB2 with spinal cord lysates from WT and *Necab2*$^{-/-}$ mice using HPA013998 and HPA014144 anti-NECAB2 antibodies. Note that antibody HPA014144 has an unspecific band (asterisk) between two specific bands. Representative data from n = 2 wild-type and n = 4 *Necab2*$^{-/-}$ mice are shown. Another non-specific band occurs above 100 kDa, also indicated with asterisk. *Scale bar* = 100 µm (B).

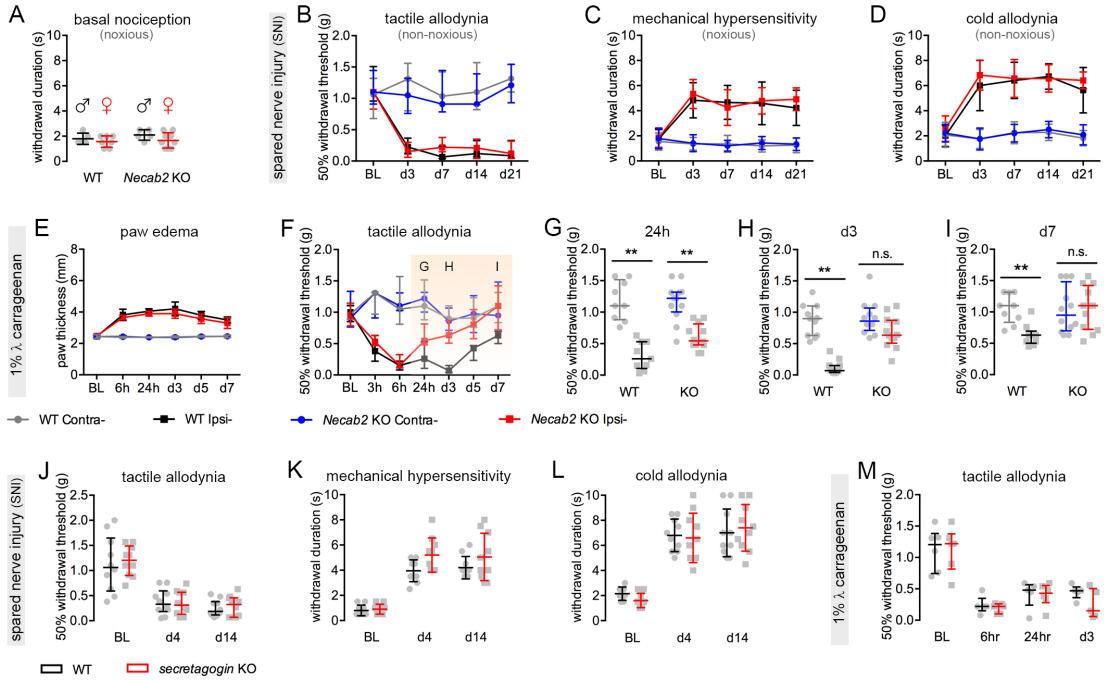

Figure 4. **Genetic deletion of NECAB2 gates inflammatory but not neuropathic pain. A.** Basal nociceptive sensation (upon noxious mechanical stimulus, pinprik) of *Necab2*$^{-/-}$ mice is intact (relative to wild-type (WT) mice) in a gender independent manner (n = 5 – 9/group). **B-D**. After SNI, *Necab2*$^{-/-}$ mice develop tactile allodynia (von Frey filaments, innocuous stimulus), mechanical hypersensitivity (noxious mechanical stimulus) and cold allodynia (acetone stimulus) equivalent to their WT counterparts (n = 12 for WT and n = 14 for *Necab2*$^{-/-}$ mice of both sexes). **E**. Time course of edema to the hind-paw, the typical symptom of inflammation, for WT and *Necab2*$^{-/-}$ mice (n > 8/time point/group) after intraplantar injection of λ carrageenan (1%, 20 µl). **F**. Time-course of tactile allodynia after λ carrageenan application differs between *Necab2*$^{-/-}$ and WT mice: **G-I**. Differential responses in the von Frey filament test after inflammation. Note the rapid behavioral recovery upon *Necab2* deletion. **J-L**. After SNI, secretagogin null (*Scgn*$^{-/-}$) mice (all male) develop tactile allodynia, mechanical hypersensitivity and cold allodynia that are indistinguishable from WT littermates (n = 10/group). **M**. Likewise, *Scgn*$^{-/-}$ and wild-type mice develop tactile allodynia similarly upon λ carrageenan-induced inflammation (n = 6/group). Error bars in black and red correspond to WT and *Scgn*$^{-/-}$ mice, respectively. BL: basal level. Behavioral data lacking normal distribution were presented as medians ± interquartile ranges and statistically assessed by the Mann-Whitney test (e.g. von Frey filament test). Results of other behavioral assays (e.g., pinprick and acetone stimuli) were expressed as means ± S.D. and statistically evaluated using Student's t-test. *p < 0.05, **p < 0.01.

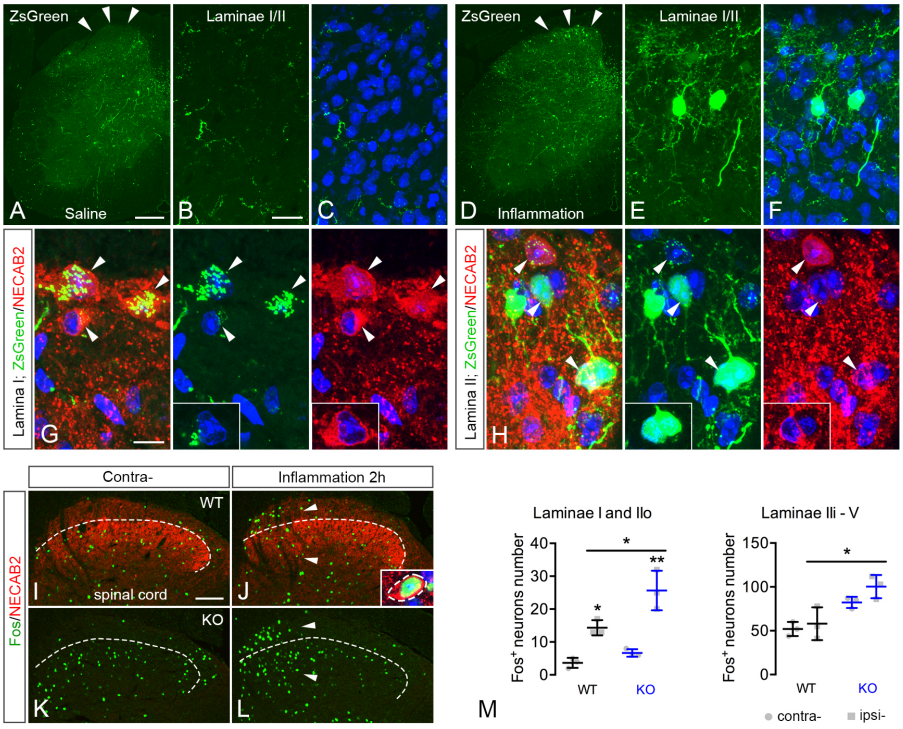

Figure 5. **Genetic dissection of spinal neuron activity upon inflammatory pain**. **A-F**. Distribution of *ZsGreen*$^{+}$ cells in spinal superficial layers from *Arc-CreERT2::Rosa26-stop-ZsGreen* 'TRAP' mice upon saline or λ carrageenan infusion. Tamoxifen was administered for 3 consecutive days after stimulation. Propidium iodide was used as nuclear counterstain. Arrowheads in A,D pinpoint the location of ZsGreen^{+} neurons in medial spinal superficial layers. **G,H**. High-resolution analysis of ZsGreen showed that these cells are NECAB2^{+} (*arrowheads*) in laminae I and II. Propidium iodide was used as nuclear counterstain. Projection images rendered from 9 and 12 μm orthogonal stacks in G and H, respectively, are shown. Insets are single-plane images selected from each deck. **I-L**. Fos^{+} cells in spinal dorsal horn 2h after λ carrageenan stimulation of wild-type (WT) and *Necab2*$^{-/-}$ (KO) mice. Dashed lines label the border between the outer (II_o) and inner (II_i) layers of lamina II. Arrowheads indicate the medial superficial dorsal horn and lamine III/IV. Inset confirms co-localization of Fos and NECAB2. **M.** Quantification of Fos^{+} neurons per section in medial laminae I/II_o and laminae II_i-V at the level of lumbar segments 4 and 5; n = 3 animals/group/genotype. Two-way ANOVA with Tukey's *post-hoc* test was performed with *$p < 0.05$, **$p < 0.01$. Data were expressed as means ± S.D. *Scale bars* = 200 μm (A,B), 100 μm (I-L), 20 μm (B,C,E,F) and 10 μm (G,H).

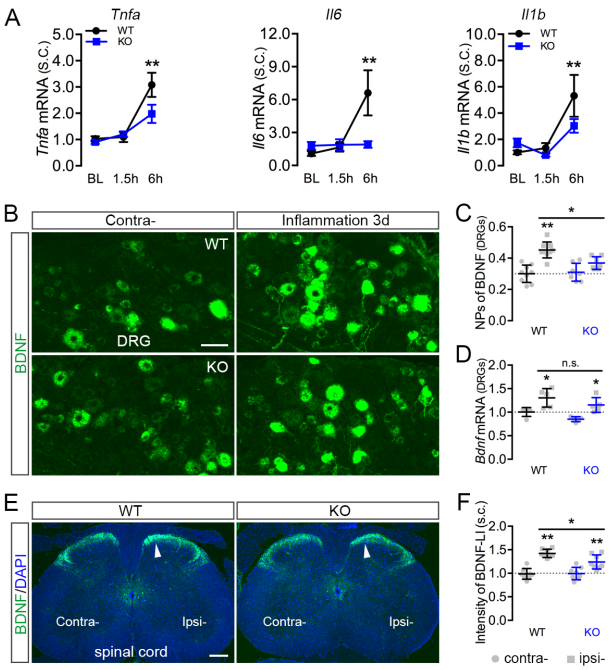

Figure 6. **Reduced pro-inflammatory cytokine and BDNF signaling in *Necab2*$^{-/-}$ mice. A**. Inflammation-induced increases in *Tnfa*, *Il6* and *Il1b* mRNA expression in the spinal cord is diminished by the genetic ablation of *Necab2* (KO; n = 15 animals/genotype). Two-way ANOVA revealed a significant inflammation × genotype interaction [$F_{(2,24)}$ = 5.491, p = 0.0109] for *Il6* after 6h of inflammation. **B**. BDNF-like immunoreactivity in DRGs from wild-type (WT) and *Necab2*$^{-/-}$ (KO) mice after 3 days of inflammation. **C**. Quantification of BDNF^{+} NPs in DRGs (n = 5 animals/genotype). Two-way ANOVA revealed significant inflammation × genotype interaction ($F_{(2,28)}$ = 6.460, p = 0.0169 (*) with group-wise comparisons returning a significant reaction for WTs (**p < 0.01, contralateral *vs.* ipsilateral). **D**. *Bdnf* mRNA in DRGs. Note the similar response in *Necab2*$^{-/-}$ mice. **E,F**. BDNF-like immunoreactivity in spinal cord after 3 days of inflammation (E) and its quantitative analysis (F). Arrowheads indicate the medial spinal superficial layers ipsilaterally. **F**. Two-way ANOVA revealed a significant inflammation × genotype interaction [$F_{(1,28)}$ = 4.694, p = 0.0389]; n = 9 for wild-type and n = 8 for *Necab2*$^{-/-}$ mice. *p < 0.05, **p < 0.01. Data were expressed as means ± S.D. *Abbreviations:* contra-, contralateral; ipsi-, ipsilateral; n.s., non-significant. *Scale bars* = 200 μm (E), 50 μm (B).

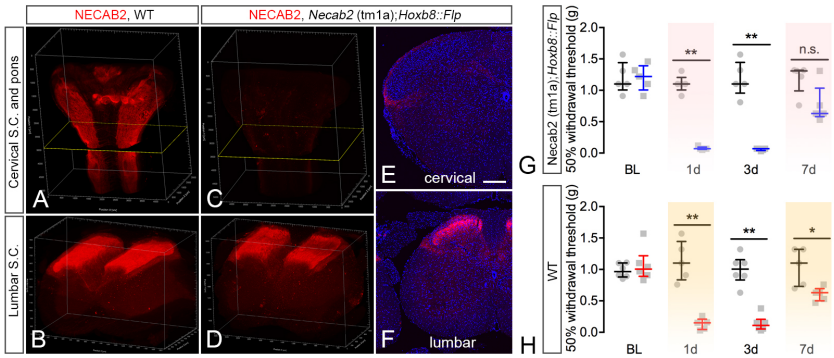

Figure 7. **Genetic rescue of *Necab2* at the spinal level reinstates tactile allodynia after inflammation. A-D**. Graphical rendering of three-dimensionally reconstructed intact tissues after NECAB2 immunohistochemistry using iDISCO^{+} and subsequent light-sheet microscopy. Pons-cervical spinal cord (S.C.) and lumbar S.C. are shown from both wild-type (WT; A,B) and *Hoxb8-Flp::Necab2*(tm1a) mice (C,D). Note that *Hoxb8* expression is restricted to spinal cord and DRG. **E,F**. NECAB2 histochemistry in transverse sections of cervical (E) and lumbar (F) spinal cord from *Hoxb8-Flp::Necab2*(tm1a) mice. Individual planar sections are shown at anatomical coordinates corresponding to panels C and D, respectively. Sections were counter-stained with DAPI. **G,H**. *Hoxb8-Flp::Necab2*(tm1a) mice (n = 5) develop tactile allodynia after peripheral inflammation (von Frey filament test) to an extent similar to that seen in WT mice (n = 6), even if NECAB2 is not expressed supraspinally. Data were expressed as medians ± interquartile ranges and statistically evaluated by the Mann-Whitney U test. *p < 0.05, **p < 0.01. *Abbreviations*: BL, baseline; d, day; ns, non-significant. *Scale bar* = 250 µm in (E).